A Time-Scale Adaptive Dispatch Method for Renewable Energy Power Supply Systems on Islands

Canbing Li, Senior Member, IEEE, Xubin Liu, Student Member, IEEE, Yijia Cao, Senior Member, IEEE, Peng Zhang, Senior Member, IEEE, Haiqing Shi, Student Member, IEEE, Lingyu Ren, Student Member, IEEE, and Yonghong Kuang

Abstract—A salient feature of a renewable energy power supply system (REPSS) on islands is the high level of uncertainties caused by high penetration of volatile power sources, such as wind and solar photovoltaic farms. This creates large forecast errors under some conditions and makes the fixed time-scale dispatch impotent in maintaining system reliability. To tackle this challenge, a time-scale adaptive dispatch method is developed in this paper. The time-scale for dispatch REPSS on islands is adjusted online according to the confidence interval of forecast error predicted by neural network. Extensive tests have validated the effectiveness of the presented method in offsetting the uncertainties in the system and improving the system reliability.

Index Terms—Energy management system, forecast, microgrid, reliability, spinning reserve capacity.

I. Introduction

RENEWABLE energy power supply system (REPSS) is an emerging paradigm for electrifying small and medium-sized power systems on islands [1]. It is a real-life hybrid system integrating renewable sources such as wind power, solar photovoltaic (PV), and ocean current generation, with stabilizing resources including diesel generators and batteries [2], [3]. REPSS becomes an increasingly appealing off-shore energy solution because it takes advantage of the immediately available renewables offering clean energy consumption and low carbon footprint [4].

REPSS on islands is actually a special type of microgrid. Different from other microgrids, REPSS has the following features

1) REPSS has high penetration of renewable generation (sometimes near 100%), causing highly intermittent and uncertain operational conditions [5].

Manuscript received June 16, 2014; revised May 5, 2015 and August 8, 2015; accepted September 25, 2015. Date of publication October 19, 2015; date of current version February 17, 2016. This work was supported in part by the National High Technology Research and Development Program of China (863 Program) under Grant 2011AA050203, and in part by the U.S. National Science Foundation under Grant CNS-1419076. Paper no. TSG-00601-2014.

C. Li, X. Liu, Y. Cao, H. Shi, and Y. Kuang are with the College of Electric and Information Engineering, Hunan University, Changsha 410082, China (e-mail: licanbing@qq.com; yjcao@hnu.edu.cn).

P. Zhang and L. Ren are with the Department of Electrical and Computer Engineering, University of Connecticut, Storrs, CT 06269-2157 USA (e-mail: peng@engr.uconn.edu).

Color versions of one or more of the figures in this paper are available online at http://ieeexplore.ieee.org.

Digital Object Identifier 10.1109/TSG.2015.2485664

- 2) REPSS normally operates in the islanding mode, which means the reliability is of top priority. On the other hand, land-based microgrids might mainly operate in the gridconnected mode, which take the economical operation as their prioritized objective [6].
- 3) REPSS is frequently exposed to extreme weather and natural disasters (e.g., typhoon and tsunami).

As a comparison, grid-connected microgrids usually operate under normal conditions [7]. Therefore, dealing with uncertainties is a major challenge for the energy management in REPSS. The analysis methods of REPSS can draw on the experience of traditional microgrids technology.

Extensive research has been conducted to deal with fluctuating loads and random renewable generation in microgrid for reliable and economical operation. References [8] and [9] aim to increase the accuracy of load forecast in microgrid while [10] focuses on improving the forecast of renewable generation. Reference [11] quantifies forecast errors. A stochastic optimal power flow suited for short-term operation is developed in [12] considering forecast errors for renewable generation. Optimal allocation of energy storage is presented to offset the effect of variable generation [13]. Unit commitment [14] and economic dispatch are studied to cope with uncertainties in microgrid [15], [16].

Recent research shows that the multitime-scale dispatch could be an effective strategy to tackle the challenges caused by load and generation uncertainties. Originally, multitime-scales were introduced to capture long-term dynamics and short-term dynamics in power systems [17]. Recently, this philosophy was introduced to develop more realistic dispatch strategies for transmission system under uncertain environment, with more time-scale dispatch schedules being introduced [18]. For instance, a weekly dynamic rolling approach has been used to coordinate long-term and short-time wind generation scheduling [19]. Similar approach has been implemented for dispatch thermal units [20] and interruptible loads [21]. However, all these approaches adopt a few fixed time-scales predetermined for different scenarios.

In this paper, a time-scale adaptive dispatch method is developed to achieve reliable and economic dispatch for island-based REPSS. The major contribution is an automatic adjustment method that determines the look-ahead dispatch horizon along the timeline based on the confidence coefficient

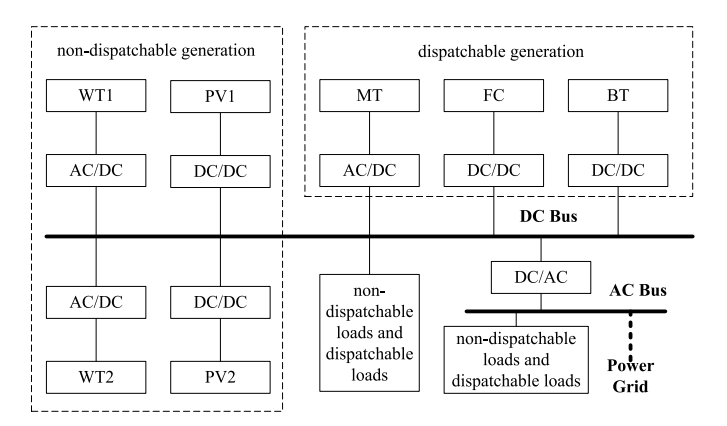


Fig. 1. Schematic of REPSS on islands.

and confidence interval of forecast error. With the dynamic time-scale adjustment, higher system reliability of REPSS is achieved under uncertain and even extreme situations.

The rest of the paper is organized as follows. The influence of confidence interval of forecast error is introduced in Section II. An adaptive adjustment method for time-scales dispatch is described in Section III. Comparative studies between the adaptive time-scale approach and the traditional fixed time-scale dispatch are provided in Section IV. The paper is concluded in Section V.

II. INFLUENCE OF FORECAST ERROR ON REPSS

A large degree of forecast error could occur in REPSS because of high levels of uncertainties in load and nondispatchable renewable generation. Obviously, an effective dispatch schedule depends on a credible forecast. Therefore, it is important to measure the degree of forecast error so that effective measures could be taken to decide an appropriate time-scale in system dispatch. Here, the confidence coefficient and confidence interval are adopted to assess the credibility level of forecasts error.

A. Confidence Coefficient and Confidence Interval of Forecast Error

The loads in REPSS can be classified into nondispatchable loads and dispatchable loads. Here the dispatchable loads include the interruptible and deferrable load (such as heating load and seawater desalination). Similarly, REPSS generation can be divided into nondispatchable and dispatchable generation. Intermittent renewable sources including wind turbine (WT) and PV generator belong to the former category, while micro turbine (MT), fuel cell (FC) and storage battery (BT) normally belong to the latter. A typical structure of REPSS is given in Fig. 1. The uncertainties mainly come from the load and nondispatchable renewable generation, and shutdown of dispatchable generation caused by faults.

Obviously, the major sources of forecast error are the nondispatchable load and the nondispatchable renewable generation. If we treat the nondispatchable generation as negative load, the equivalent nondispatchable load (we use "equivalent load" for brevity) can be expressed as follows:

$$LG_{f,t} = L_{f,t} - G_{f,t} = L_{f,t} - (W_{f,t} + PV_{f,t})$$
 (1)

$$LG_{a,t} = L_{a,t} - G_{a,t} = L_{a,t} - (W_{a,t} + PV_{a,t})$$
 (2)

where $LG_{f,t}$ and $LG_{a,t}$ are the forecast and actual equivalent load at time t, respectively, $L_{f,t}$ and $G_{f,t}$ are the forecast load and nondispatchable generation at time t, respectively, $W_{f,t}$ and $PV_{f,t}$ are the forecast wind power and solar power at time t, respectively, $L_{a,t}$ and $G_{a,t}$ are the actual load and nondispatchable generation at time t, respectively, $W_{a,t}$ and $PV_{a,t}$ are the actual wind power and solar power at time t, respectively.

The confidence coefficient and confidence interval of the forecast error are then estimated by

$$\alpha = p\{|LG_{f,t} - LG_{a,t}| \le LG_{c,T}\}\tag{3}$$

where α is the confidence coefficient of forecast error for the equivalent load during time-scale T, $p\{\bullet\}$ is the probability of $\{\bullet\}$, $LG_{c,T}$ is the confidence interval of forecast error for the equivalent load during time-scale T.

Notice that $\alpha \in (0, 1)$. For a given confidence coefficient, the value of confidence interval implies the following.

- A small confidence interval corresponds to concentrated forecast errors, meaning a low degree of uncertainties.
- A large confidence interval corresponds to well dispersed forecast errors, meaning a high degree of uncertainties.

B. Influence of Confidence Interval on the Power System Reliability

In order to ensure the system reliability, a certain reserve capacity is needed to offset the forecast error. Reliability will not be compromised when the forecast error can be neutralized. When the forecast error is higher than the available reserve, a certain amount of load needs to be curtailed and the system reliability will decline.

Assume f(x) is the density function of the forecast error for the equivalent load during time-scale T. Notice that f(x) can be obtained by fitting the observed forecast error values. Here $x \in X$ is the random variable for the forecast error and X is the set of the observed forecast errors during time-scale T. Equation (3) can also be estimated as

$$\alpha = \int_{-LG_{c,T}}^{LG_{c,T}} f(x)dx. \tag{4}$$

Meanwhile

$$x = LG_{f,t} - LG_{a,t} \tag{5}$$

where x is the forecast error for the equivalent load, f(x) is the density function of the forecast error for the equivalent load under time-scale T.

The density function is supposed to be a certain distribution. The loss of load probability (LOLP) can then be expressed as

$$p_{\text{load}} = 1 - \left(\int_{-\infty}^{LG_{c,T}} f(x)dx + \int_{LG_{c,T}}^{R_{l,t}} f(x)dxz \right)$$
 (6)

where p_{load} is the LOLP and $R_{l,t}$ is the load reserve capacity at time t.

LOLP is determined by reserve capacity; however, it is also affected by the confidence interval of forecast error on the condition that the reserve capacity is certain while the forecast error is uncertain. As can be seen from (6), for given confidence coefficient and available reserve capacity, the confidence interval of forecast error $LG_{c,T}$ can be calculated according to (4) when obtain the density function of the forecast error, then $\int_{-\infty}^{LG_{c,T}} f(x) dx$ in (6) can be acquired. Because $\int_{-\infty}^{LG_{c,T}} f(x) dx$ is determined by the confidence coefficient, LOLP is affected by $\int_{LG_{c,T}}^{R_{l,t}} f(x) dx$, which becomes small when the confidence interval is large. As a result, large confidence interval leads to high LOLP.

On the other hand, the spinning reserve is normally used as both the load reserve and the emergency reserve to offset the power shortage caused by random events in REPSS. Here the random events include the forced outage of dispatchable generators and the forecast error of the equivalent load. The system reliability can then be expressed as [22]

$$1 - \gamma = \left(\prod_{i=1}^{m} (1 - \lambda_i)\right)$$

$$\times \left(1 - \left(\int_{-\infty}^{LG_{c,T}} f(x)dx + \int_{LG_{c,T}}^{R_{s,t}} f(x)dx\right)\right)$$

$$+ \sum_{i=1}^{n} \lambda_i \left(\prod_{j=1, j \neq i}^{m} (1 - \lambda_j)\right)$$

$$\times \left(1 - \left(\int_{-\infty}^{LG_{c,T}} f(x)dx + \int_{LG_{c,T}}^{R_{s,t} - P_{i,\max}} f(x)dx\right)\right)$$
(7)

where γ is the system reliability, m is the number of dispatchable generators, n is the number of dispatchable generators unavailable due to forced outages, λ_i is the forced outage rate of dispatchable generator i, $R_{s,t}$ is the spinning reserve capacity at time t, and $P_{i,\max}$ is the maximal output of the ith dispatchable generator.

It can similarly be inferred from (6) that, when the spinning reserve capacity is only provided by the available reserve capacity, large confidence interval of forecast error leads to low power supply reliability.

C. Influence of Confidence Interval on the Economic Operation of Power System

The confidence interval of forecast error also influences the economic operation of power system.

For fixed system reliability and confidence coefficient, the spinning reserve capacity and confidence interval shall vary together in order to keep $\int_{LG_{c,T}}^{R_{s,t}} f(x) dx$ or $\int_{LG_{c,T}}^{R_{s,t}-P_{i,\max}} f(x) dx$ constant, as shown in (6) and (7). This means that a large confidence interval leads to a high level of required spinning reserve capacity. Large confidence interval, therefore, increases the operational costs of power system.

III. TIME-SCALE ADJUSTMENT FOR ADAPTIVE DISPATCH

When the spinning reserve for offsetting the forecast error is in excess of the available reserve, the spinning reserve could no longer compensate for the excessive forecast error, leading to unreliable operation or even blackout. In this case, the confidence interval has to be reduced in order to decrease the spinning reserve requirement to an acceptable level. (In this paper, the spinning reserve requirement refers to the required capacity of spinning reserve to ensure a certain level of system reliability, e.g., 0.98.) Therefore, we need to search for a threshold, a maximum tolerable confidence interval for the system, which can then be required to determine whether the time-scale would be adjusted in certain situations.

A. Threshold for Confidence Interval of Forecast Error

The procedure to find the threshold for confidence interval of forecast error is elaborated as below.

The available reserve refers to the total reserve provided by the dispatchable generators and it can be estimated by

$$R_{a,t} = \sum_{i=1}^{m} S_{i,t} (P_{i,\max} - P_{i,t})$$
 (8)

where $R_{a,t}$ is the available reserve at time t, $S_{i,t}$ is the operational state of the ith dispatchable generators at time t (0 for turn off, 1 for turn on) and $P_{i,t}$ is the planned output of the ith dispatchable generators at time t.

The power balance constraints can be expressed as

$$\sum_{i=1}^{m} S_{i,t} \times P_{i,t} = L_{f,t} - W_{f,t} - PV_{f,t}. \tag{9}$$

Based on (1), (8) can also be expressed as

$$R_{a,t} = \sum_{i=1}^{m} S_{i,t} \times P_{i,\max} - LG_{f,t}.$$
 (10)

In general, the number of dispatchable generators which are turned on (e.g., as shown in Figs. 5 and 6) should be as less as possible. The operational state of dispatchable generators is determined as follows.

- An operation priority of dispatchable generators from high to low is set based on engineering practice in order to determine the number of dispatchable generators which are turned on (e.g., the operation priority of dispatchable generators is set as MT1>FC1>BT>MT2>FC2).
- If the calculation of adaptive time-scale has no solution, more dispatchable generators should be turned on in terms of their operation priority in order to increase the available reserve.

Once the operational states of dispatchable generators are made, the threshold for confidence interval of forecast error $LG_{c,\max}$ could be assessed considering two different scenarios.

 The available reserve is inadequate to meet the spinning reserve requirement. In this situation, power system operates with low reliability. The spinning reserve is provided by the minimum available reserve

$$R_{s,t} = \min_{t=1}^{T_a} R_{a,t}$$
 (11)

where T_a is the adaptive time-scale. Substitute $R_{s,t}$ into (7), for a given reliability level γ , $LG_{c,T}$ could be obtained. This value is the threshold of confidence interval, also denoted as $LG_{c,\max}$.

2) The available reserve is able to satisfy the spinning reserve requirement. In this situation, the spinning reserve is equal to the minimum available reserve

$$R_{s,t} = \min_{t=1}^{T_s} R_{a,t}$$
 (12)

where T_s is the fixed time-scale.

Similar to Scenario 1, the threshold for confidence interval of forecast error can be obtained by using (7), that is, the obtained $LG_{c,T}$ is also denoted as $LG_{c,\max}$.

A time-scale is divided into a number of time periods. In this paper, the spinning reserve is determined by the minimum available reserve of one time period during a time-scale. If the minimum available reserve can meet the requirement, other time periods can meet the requirement even better. Therefore, the available reserve in this time-scale can meet the spinning reserve requirement.

B. Adaptive Adjustment of Dispatch Time-Scale

The prediction for confidence interval of forecast error for the equivalent load during time-scale T ($LG_{c,f}$) can be predicted by a neural network (NN) detailed in the Appendix. For a given confidence coefficient, the prediction for the confidence interval of forecast error will vary in response to the changes in ambient environment. When ambient environment becomes harsh, the confidence interval would increase. Then it is necessary to reduce time-scale. When the available reserve is equal to or larger than the spinning reserve requirement, the time-scale would remain unchanged. Below elaborates how the time-scale is adjusted under different scenarios.

Scenario 1: The relationship between the prediction for confidence interval of forecast error $LG_{c,f}$ and the threshold for confidence interval of forecast error $LG_{c,\max}$ is satisfied the following conditions:

$$LG_{c,f} \le LG_{c,\max}.$$
 (13)

When the prediction for confidence interval of forecast error $LG_{c,f}$ is equal to or less than the threshold for confidence interval of forecast error $LG_{c,\max}$, this means the environment is "friendly" because the system has sufficient available reserve and can withstand higher forecast error. For this case, we choose to keep the time-scale unchanged; otherwise it would result in frequent adjustment during the dispatch.

Scenario 2: The relationship between the prediction for confidence interval of forecast error $LG_{c,f}$ and the threshold for confidence interval of forecast error $LG_{c,\max}$ is satisfied the following conditions:

$$LG_{c,f} > LG_{c,\max}.$$
 (14)

If (14) holds, the time-scale would be reduced, otherwise the available reserve would be insufficient.

The time-scale adjustment is performed by the NN from the Appendix. A group of historical data (e.g., 5-day data) is used to train the NN in order to obtain the NNs connection weights

with a fixed time-scale value T_s (e.g., 6 h). Then the trained NN is employed to adaptively adjust the time-scale T_a

$$T_a = k \times T_s \tag{15}$$

where k is the adjustment coefficient.

The time-scale is changed every 5 min in Scenario 2. The step of adjustment coefficient refers to the change size of the adjustment coefficient every time in order to change the time-scale every 5 min. Therefore, the step of adjustment coefficient is expressed as

$$J = \frac{5 \text{ min}}{T_s \times 60 \text{ min}} = \frac{1}{12 \times T_s} \tag{16}$$

where J is the step of adjustment coefficient [e.g., (1/72) when the fixed time-scale is 6 h].

The adjustment coefficient k is changed as follows.

Scenario 1: The time-scale is unchanged

$$k = 1. (17)$$

Scenario 2: The time-scale would be reduced

$$k = J \times h$$
 $h = 1, 2, 3, \dots, H$ (18)

where h is the number of times to change the adjustment coefficient. H is the total number of times (e.g., the maximum value of H is 72).

Sometimes, it is hard to make the $LG_{c,f}$ based on NN just equal to the $LG_{c,\max}$, with the increase of h, the time-scale aims to satisfy

$$\eta \times LG_{c,\max} \le LG_{c,f} \le LG_{c,\max}$$
(19)

where η is the judgment coefficient close to 1. At this time-scale, the prediction for confidence interval of forecast error $LG_{c,f}$ is just equal to or a bit less than the threshold for confidence interval of forecast error $LG_{c,\max}$.

In Scenario 2, the time-scale is constantly changed with respect to the corresponding wind speed, solar radiation, fore-cast method, and day types (see the Appendix); when the prediction for confidence interval of forecast error $LG_{c,f}$ and the threshold for confidence interval of forecast error $LG_{c,\max}$ firstly satisfy (19), T_a is kept unchanged, and then goes to next dispatch schedule.

The above procedure for adaptively adjusting dispatch time-scale is illustrated in Fig. 2.

The developed time-scale adaptive dispatch method is particularly suitable for look-ahead dispatch [23], [24], which makes dispatch schedules for future horizons ranging from minutes to hours.

It is worth noting that not all the scheduled points will be fully executed within a time-scale. To better follow the industry practices, the dispatch schedule is triggered according to the following situations.

- 1) New dispatch schedule should be worked out when the current dispatch schedule is near the end. In order to facilitate the transition, the new dispatch schedule is worked out when the current scheduled points are executed at 80% of its whole cycle $(0.8 \times T_a)$.
- Considering the high volatility in the REPSS, the new dispatch schedule should be worked out immediately

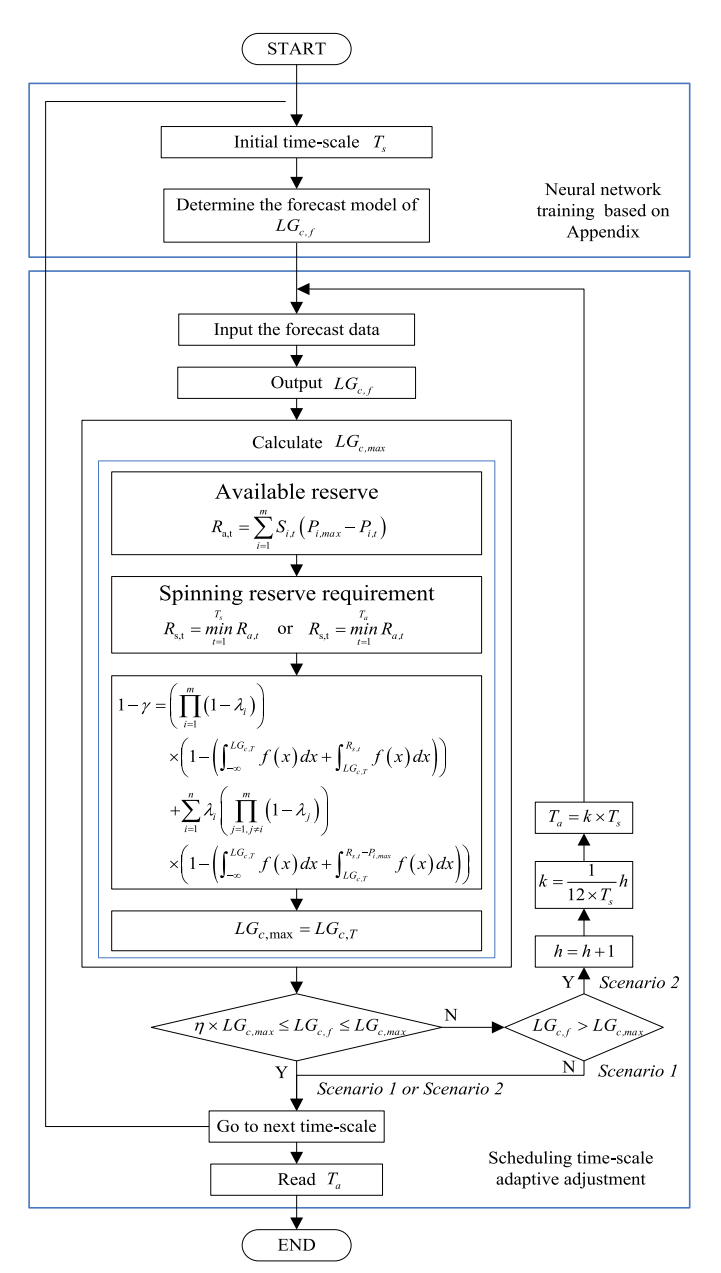


Fig. 2. Prediction for confidence interval of forecast error and adaptive adjustment of dispatch time-scale.

when there is a large deviation between the actual operation situation and the planed operation situation. For example, the system has a transition between island mode and grid-connected mode, the unit operation state is different from the dispatch schedule.

To summarize, not all the scheduled points will be executed in practice, and the reschedule of dispatch should be considered. However, those unexecuted points could still be useful. On the one hand, how many scheduled points will be not executed in practice is unknown in advance. On the other hand, it is beneficial to connect the current dispatch schedule to the next dispatch schedule since the planed dispatch schedule has a longer time horizon than practical dispatch schedule. So as to avoid condition that the dispatchable resources are exhausted in current dispatch schedule and make the next dispatch schedule infeasible or has a low optimization level.

C. Economy Analysis of Spinning Reserve

The spinning reserve is mainly aimed at improving the system reliability and reducing the power loss. However, it cannot be taken for granted that the more spinning reserve, the better.

- If the spinning reserve is insufficient, it would be difficult to meet the load demand, thus resulting in a lack of ability to deal with emergencies. It is not conducive to the safe and economical operation of power system, as it reduces the system reliability and increases the unreliability cost.
- 2) If the spinning reserve is redundant, the reliability of the system would be improved. However, some spinning reserve will be idle and do not really participate in practical scheduling to balance load, leading to the waste of reserve resources and the increase of operation costs.

The spinning reserve will not bring direct economic benefits, if it does not participate in the practical dispatch schedule. Because the REPSS is far from main grid and mainly operates in island mode, one mainly considers the fuel cost (assume all the spinning reserve participates in practical scheduling) but do not consider the opportunity cost between REPSS and the main grid.

The economic problem of spinning reserve is the total cost of dispatchable generators which satisfy the operation constraints of power system in a time-scale. Therefore, it can be formulated as follows:

$$A_{i,t} = a_i (P_{i,t} + F_{i,t})^2 + b_i (P_{i,t} + F_{i,t}) + c_i$$
 (20)

$$B_{i,t} = a_i P_{i,t}^2 + b_i P_{i,t} + c_i (21)$$

$$C_{i,t} = A_{i,t} - B_{i,t} (22)$$

where $A_{i,t}$ is the cost of *i*th dispatchable generator after considering the spinning reserve at time t, $B_{i,t}$ is the cost of *i*th dispatchable generator before considering the spinning reserve at time t, $C_{i,t}$ is the cost of *i*th dispatchable generator for provide spinning reserve at time t, a_i , b_i , and c_i are the cost coefficient of *i*th dispatchable generator, and $F_{i,t}$ is the spinning reserve of *i*th dispatchable generator at time t.

The objective function about economy of spinning reserve under the reliability is estimated as follows:

$$\min \sum_{t=1}^{T} \sum_{i=1}^{m} C_{i,t}.$$
 (23)

IV. CASE STUDY

A. System Data

The test case consists of 550 kW nondispatchable generation composed by a 200 kW PV farm and a 350 kW WT. The dispatchable generators include two micro gas turbines, two FCs and a BT. Table I summarizes the system parameters, which are adopted from [25]. Here confidence coefficient α is 0.96, power system reliability γ is 0.98, and judgment coefficient η is 0.98.

Forecast error of load, wind power, and PV can be expressed by zero mean normal distribution as shown in [26]–[28]. Assuming that the forecast errors of loads and nondispatchable renewable generation are unrelated, the total forecast error

TABLE I PARAMETERS FOR THE TEST REPSS

Power source	PV	WT	MT1	MT2	FC1	FC2	BT
Minimum output (kW)	0	0	10	5	4	3	-30
Maximal output(kW)	40	50	100	80	80	30	30
Ramp rate(kW/h)	*	*	180	160	160	150	200
Forced outage rate	0.003	0.04	0.01	0.006	0.006	0.015	0.002
$a(Y/kW^2h)$	0.03	0.06	0.04	0.05	0.03	0.035	0.05
b(Y/kWh)	0	0	0.26	0.3	0.2	0.225	0
c (Y/h)	0	0	7	6.1	12	7.5	0
Number	5	7	2	1	1	1	1

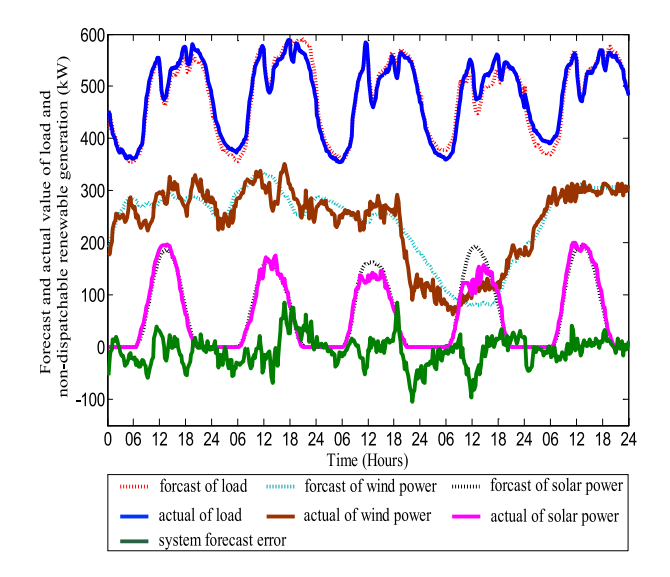


Fig. 3. Forecast and actual of load and nondispatchable generation during five days.

of the equivalent load in REPSS can be modeled by normal distribution function.

The 5-day forecast and actual values of load and nondispatchable renewable generation are illustrated in Fig. 3.

B. Dispatch Schedules With Fixed and Adaptive Time-Scale

The probability of losing two or more generators simultaneously is very low. Therefore, it is assumed that only one unit (e.g., one of MT1) may have forced outage ($S_{i,t} = 0$).

Fig. 4 shows the forecasted load and nondispatchable renewable generation in the sixth day.

Initially, a fixed time-scale T_s is set to be 6 h in the study. An optimization algorithm (optimal power flow based on particle swarm optimization) is applied for dispatch schedule to account for uncertainties to the balance of reliability and economy. On the condition of reliability, and considering the relevant operation constraints (power balance constraints, generator output constraint, spinning reserve constraints, and ramp rate constraints), the optimization algorithm is intent to iteratively search the global optimal solution for the purpose of spinning reserve economy. In addition, when a certain time-scale is made, some other optimization methods can also

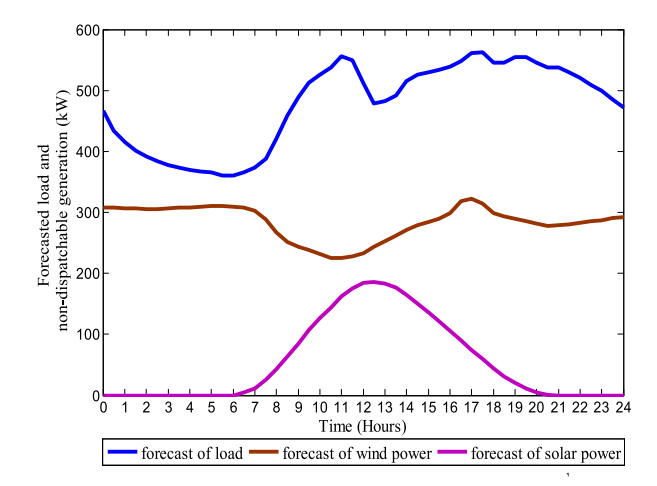


Fig. 4. Forecasted load and nondispatchable generation in the sixth day.

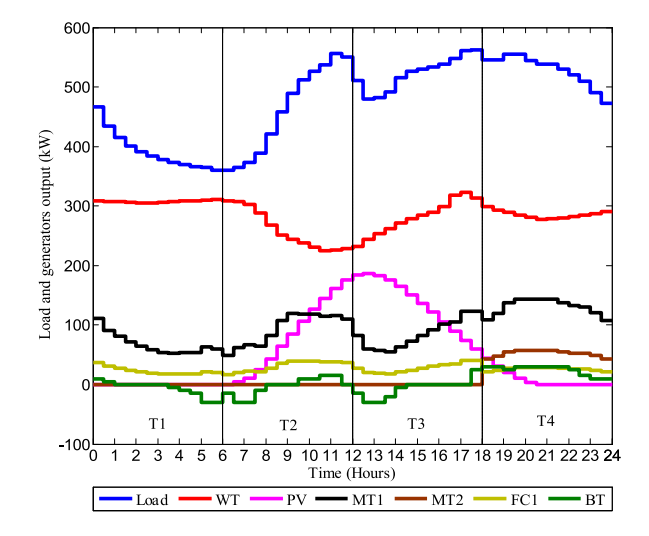


Fig. 5. Dispatch schedules with a fixed 6 h time-scale.

TABLE II

CONFIDENCE INTERVAL AND RESERVE CAPACITY WITH
A FIXED DISPATCH TIME-SCALE OF 6 h

Fixed time-scale	$LG_{c,f}$ (kW)	$LG_{c,max}$ (kW)	Е	Needed $R_{s,t}$ (kW)	Minimum $R_{a,t}$ (kW)
T ₁ (00:00-06:00)	32.22	51.51		132.34	151.26
T ₂ (06:00-12:00)	77.46	41.20	-88.01%	177.08	141.03
T ₃ (12:00-18:00)	66.95	20.67	-223.90%	166.63	120.57
T ₄ (18:00-24:00)	29.98	30.25		129.11	130.09

be used to work out the dispatch schedule, such as robust optimization method or interval-based method [29]–[33].

Based on the forecast data in Fig. 4, the dispatch schedules of load and generators with the fixed time-scale are shown in Fig. 5. It can be observed that the dispatch constraints have been considered in the study. Also, it can be seen from Fig. 5 that the time-scale and time interval are fixed all the time when dispatch time-scale is adopted. And the test system is dispatched four times per day.

Time-scale before adjustment	$LG_{c,f}$ (kW)	$LG_{c,max}$ (kW)	E	Time-scale after adjustment	$LG_{c,f}$ (kW)	$LG_{c,max}$ (kW)	Е	Needed $R_{s,t}$ (kW)	Minimum $R_{a,t}$ (kW)
T ₁ 00:00-06:00	32.22	51.51		T ₁ 00:00-06:00	32.22	51.51		132.34	151.26
T ₂ 06:00-12:00	77.46	41.20	-88.01%	T ₂ 06:00-09:00	65.39	66.72	1.99%	166.31	166.52
T ₃ 09:00-15:00	61.85	41.20	-50.12%	T ₃ 09:00-12:30	40.61	41.20	1.43%	140.93	141.10
T ₄ 12:30-18:30	60.11	20.67	-190.80%	T ₄ 12:30-17:30	45.38	46.20	1.77%	145.86	145.98
T ₅ 17:30-23:30	50.92	20.67	-146.35%	T ₅ 17:30-18:00	20.27	20.67	1.94%	120.32	120.57
T ₆ 18:00-24:00	29.98	30.25		T ₆ 18:00-24:00	29.98	30.35		129.11	130.09

TABLE III
CONFIDENCE INTERVAL AND RESERVE CAPACITY WITH ADAPTIVE DISPATCH TIME-SCALE

The confidence intervals and reserves with fixed dispatch time-scale are shown in Table II.

It can be observed from Table II that the forecasted confidence interval is less than the threshold in dispatch time-scale T_1 , larger than that in dispatch time-scale T_2 , T_3 , and a little less than that in dispatch time-scale T_4 when the fixed time-scale is adopted. The relative error E (detailed in the Appendix and considered in Scenario 2) is quite unstable under fixed time-scale. Spinning reserve requirements are related to forecasted confidence interval. When the forecasted confidence interval is large than threshold, it means the available reserve is insufficient. When the forecasted confidence interval is equal to or less than threshold, it means the available reserve is sufficient.

As a comparison, the confidence intervals and reserves with the adaptive dispatch time-scales are summarized in Table III.

It can be observed from Table III that the forecasted confidence interval is much larger than threshold before time-scale is adjusted. The relative error E is quite unstable before time-scale is adjusted, but becomes stable and smaller after time-scale is adjusted in Scenario 2. Spinning reserve requirements are related to threshold [forecasted confidence interval after time-scale adjustment should satisfy (15)]. Under the restriction of threshold, available reserve is sufficient all the time with adaptive time-scale.

By comparing Tables II and III, it can be observed that available reserve is sufficient all the time with adaptive time-scale, but, insufficient when forecasted confidence interval is large than threshold with fixed time-scale (e.g., 06:00-12:00 and 12:00-18:00). When the prediction for the confidence interval of forecast error $LG_{c,f}$ gravitates toward the threshold for confidence interval of forecast error $LG_{c,\max}$, the relative error drops to $E \in [-0.02, 0.02]$ (e.g., 06:00-09:00, 09:00-12:30, 12:30-17:30, and 17:30-18:00). Therefore, the forecast error of NN is acceptable, and the system reliability can meet the requirement after time-scale adaptive adjustment.

The dispatch schedules of loads and generators with adaptive time-scales are shown in Fig. 6.

The key point of this paper is to obtain a certain timescale after time-scales adaptive adjustment. It can be seen from Fig. 6 that the time-scales are adjusted in different scenarios.

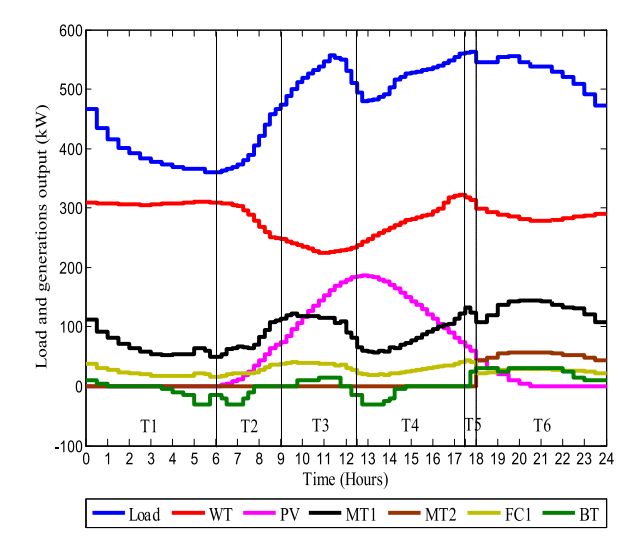


Fig. 6. Dispatch schedules with adaptive time-scales.

Meanwhile, the time intervals would be reduced when the dispatch time-scale is reduced.

By comparing Figs. 5 and 6, it can be concluded that the length of adaptive time-scale is uncertain and it can be equal to or less than fixed time-scale. The results are based on the comparison between the prediction for confidence interval of forecast error $LG_{c,f}$ and the threshold for confidence interval of forecast error $LG_{c,\max}$.

C. Comparison Between Fixed and Adaptive Dispatch Time-Scale

1) Reliability of Power System: Under the required confidence coefficient (0.96) and REPSS system reliability (0.98), the actual power supply reliabilities of the two dispatch schedules based on available reserve capacity are shown in Fig. 7. When the fixed dispatch time-scale is adopted, the actual reliability of the system is much lower than the expected value (0.98) during several time intervals (e.g., 8:30–12:00 and 17:00–18:00 under fixed time-scale). On the other hand, the actual reliability of the system is always higher than the required value when the adaptive dispatch time-scale is adopted.

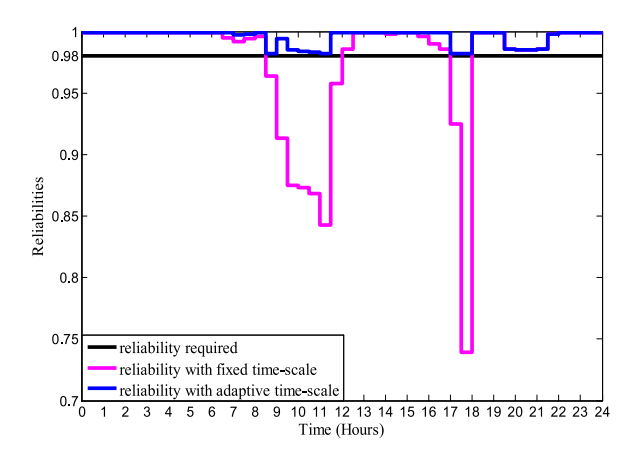


Fig. 7. Comparison of power system reliability.

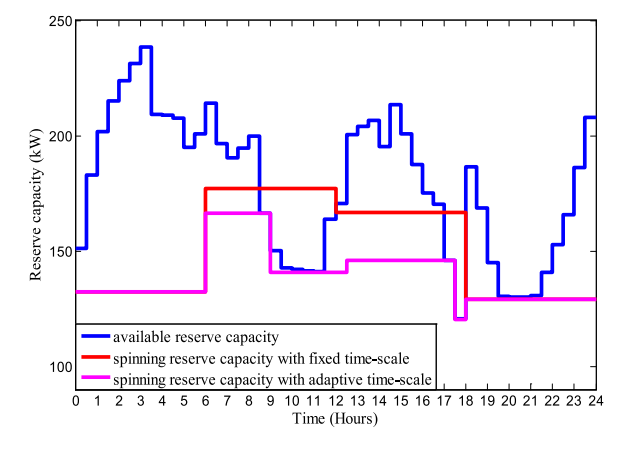


Fig. 8. Comparison of reserve requirements.

2) Economy of Power System: Under the required confidence coefficient (0.96) and power system reliability (0.98), the available reserve capacity and spinning reserve requirements with fixed and adaptive dispatch time-scale are shown in Fig. 8. Spinning reserve capacity with fixed dispatch time-scale often exceeds the available reserve capacity when actual power system reliability is lower than the required value. On the other hand, the time-scale adaptive dispatch ensures that the spinning reserve requirement is lower than the available reserve all the time.

It can be seen from the above comparisons that the time-scale adaptive dispatch can significantly improve the reliability and operational performance of REPSS where large uncertainties permeate.

Since the REPSS is far from the main grid and mainly operates in island state, an assumption is made to turn on the dispatchable generator (MT2), offsetting the load demand when the spinning reserve is insufficient, and not from main grid.

The economy comparison of spinning reserve between fixed time-scale and adaptive time-scale is shown in Table IV.

It can be observed from Table IV that: in Scenario 1, when the time-scale is equal to the fixed time-scale (e.g., 00:00–06:00 and 18:00–24:00), both the cost and average cost of spinning reserve under adaptive time-scale is equal to that in fixed time-scale. In Scenario 2, when the time-scale is reduced (e.g., 06:00–09:00, 09:00–12:30, 12:30–17:30, and 17:30–18:00), both the cost and average cost of spinning

TABLE IV
COMPARISON OF SPINNING RESERVE ECONOMY BETWEEN
FIXED TIME-SCALE AND ADAPTIVE TIME-SCALE

Fixed time-scale	Cost (Y)	Average cost (Y/h)	Adaptive time-scale	Cost (Y)	Average cost (Y/h)
T ₁ 00:00-06:00	2255.98	376.00	T ₁ 00:00-06:00	2255.98	376.00
T ₂ 06:00-12:00	3575.09	595.85	T ₂ 06:00-09:00	1248.16	416.05
T ₃ 12:00-18:00	3209.62	534.94	T ₃ 09:00-12:30	1324.93	378.55
T ₄ 18:00-24:00	2178.58	363.10	T ₄ 12:30-17:30	1934.86	386.97
			T ₅ 17:30-18:00	149.05	298.10
			T ₆ 18:00-24:00	2178.58	363.10
00:00-24:00	11219.27	467.47	00:00-24:00	9091.56	378.82

reserve under adaptive time-scale is lower than that in fixed time-scale. For the large uncertainties in REPSS on islands in a longer time horizon which contains the reduced time-scale (e.g., 00:00–24:00), both the cost and average cost of spinning reserve under adaptive time-scale could be lower than the cost of spinning reserve under fixed time-scale.

V. CONCLUSION

An effective dispatch schedule depends on a credible forecast which is mainly influenced by time-scale and ambient environment. In order to improve the reliability and achieve an economic dispatch of REPSS, a time-scale adaptive dispatch method is presented to deal with the uncertainties of power and renewable power output. The confidence coefficient and confidence interval are adopted to assess the credibility level of forecasts error. It has been worked out that the time-scale of dispatch schedules for REPSS would be dynamically adjusted to improve system reliability and economy. To achieve adaptive dispatch, the prediction for confidence interval of forecast error should be forecasted at first. Then the dispatch time-scale is adjusted online by comparing the forecasted confidence interval with an appropriate threshold. The adaptive time-scale is adjusted under two different scenarios. And the length of adaptive time-scale can be equal to or less than the fixed time-scale. Comparative studies for the fixed time-scale dispatch and the adaptive time-scale dispatch are performed. The results show that the adaptive time-scale dispatch significantly dominates the fixed time-scale dispatch in terms of system reliability and spinning reserve efficiency.

The method can also be applied to other microgrids and active distribution network where there is high penetration of distributed generation.

APPENDIX PREDICTION FOR CONFIDENCE INTERVAL OF FORECAST ERROR

The method of the prediction for confidence interval of forecast error $LG_{c,f}$ based on NN is shown as follows.

The confidence interval of forecast error is an important parameter for credible and efficient system operations.

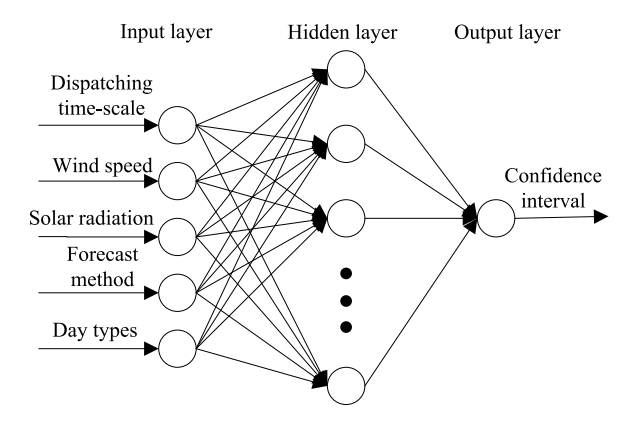


Fig. 9. NN for forecasting of the confidence interval.

Typically, predicting the confidence interval is a critical step in the time-scale adaptive dispatch schedule.

The confidence interval of forecast error is mainly influenced by the following factors.

- Time-Scale: With the growth of the time-scale, the forecast error will gradually increase, and the confidence interval will increase. The shorter the time-scale, the smaller the forecast error, and the smaller the confidence interval.
- 2) Ambient Environment (Solar Radiation and Wind Speed): Generally speaking, when ambient environment becomes harsh, the forecast error will increase and the confidence interval will increase.
- 3) Other Factors (Forecast Method and Day Types): The forecast accuracy is decreasing in the sequence of ultra short term forecast method, extended short term forecast method, and short term forecast method. The change of day types can also influence the forecast error.

Basically, the confidence interval is a highly nonlinear function of these factors. For this reason, NN can be a potent approach to predict the confidence interval.

So far, back propagation (BP) algorithm has been the most successful method for NN. Reference [34] introduces a Levenberg–Marquardt-based (LM) BP algorithm, which combines the advantages of the steepest descent method with the Gauss–Newton method and has fast convergence speed and high prediction accuracy. Therefore, the LM-based NN is adopted to predict the confidence interval.

The forecasted confidence interval can be expressed as

$$LG_{c,f} = g(T, S_{f,T}, W_{f,T}, M_T, D_T)$$
 (24)

where $LG_{c,f}$ is the prediction for confidence interval of forecast error, T is the time-scale for dispatch, $S_{f,T}$ and $W_{f,T}$ are the forecasted solar radiation and wind speed during T, respectively, M_T and D_T are the forecasted method and day types during T, respectively. Notice that more factors can be added in $g(\bullet)$ for higher granularity analysis.

The NN consists of input layer, hidden layer, and output layer [35], as shown in Fig. 9. Here the input and output vectors of the NN are expressed as follows:

$$Y = [T, S_{f,T}, W_{f,T}, M_T, D_T]$$
 (25)

$$O = \left[LG_{c,f} \right] \tag{26}$$

where *Y* and *O* are the input and output vectors, respectively. When the time-scale needs to be reduced, the forecast error of NN is estimated as follows:

$$E = \frac{LG_{c,\text{max}} - LG_{c,f}}{LG_{c,\text{max}}} \times 100\%$$
 (27)

where E is the relative error about the confidence interval of forecast error.

The threshold for confidence interval of forecast error $LG_{c,\max}$ is restricted by the available reserve. Constantly adjust the time-scale and its corresponding solar radiation, wind speed, forecast method, and day types, and until $E \in [-0.02, 0.02]$. In this way, we think that the forecast error of NN can be acceptable.

ACKNOWLEDGMENT

The authors would like to thank C. Cao, W. Liu, H. Wang, and J. Wei for their contribution to this paper, and T. Orekan for revising this paper.

REFERENCES

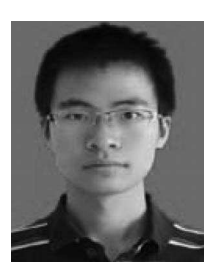
- T. Kojima and Y. Fukuya, "Microgrid system for isolated islands," FUJI Elect. Rev., vol. 57, no. 4, pp. 125–130, 2011.
- [2] T. Senjyu, D. Hayashi, A. Yona, N. Urasaki, and T. Funabashi, "Optimal configuration of power generating systems in isolated island with renewable energy," *Renew. Energy*, vol. 32, no. 11, pp. 1917–1933, 2007.
- [3] T. Senjyu, T. Nakaji, K. Uezato, and T. Funabashi, "A hybrid power system using alternative energy facilities in isolated island," *IEEE Trans. Energy Convers.*, vol. 20, no. 2, pp. 406–414, Jun. 2005.
- [4] P. Michael, K. Matthew, and O. Zitouni. (Apr. 2012). Renewable Energies for Remote Areas and Islands (Remote). [Online]. Available: http://iea-retd.org/wp-content/uploads/2012/06/ IEA-RETD-REMOTE.pdf
- [5] J. Lu and M. Niu, "Overview on microgrid research and development," in *Information Computing and Applications*, vol. 105. Berlin, Germany: Springer-Verlag, 2010, pp. 161–168.
- [6] C. Schwaegerl et al. (Dec. 2009). Report on the Technical, Social, Economic, and Environmental Benefits Provided by Microgrids on Power System Operation. EU. [Online]. Available: http://www.microgrids.eu/ documents/668.pdf
- [7] M. Pelling and J. I. Uitto, "Small island developing states: Natural disaster vulnerability and global change," *Global Environ. Change Part B*, Environ. Hazards, vol. 3, pp. 49–62, Jun. 2001.
- [8] N. Amjady, F. Keynia, X. Qing, and H. Zareipour, "Short-term load forecast of microgrids by a new bilevel prediction strategy," *IEEE Trans. Smart Grid*, vol. 1, no. 3, pp. 286–294, Dec. 2010.
- [9] L. Hernandez et al., "Short-term load forecasting for microgrids based on artificial neural networks," *Energies*, vol. 6, no. 3, pp. 1385–1408, 2013.
- [10] G. Sideratos and N. D. Hatziargyriou, "An advanced statistical method for wind power forecasting," *IEEE Trans. Power Syst.*, vol. 22, no. 1, pp. 258–265, Feb. 2007.
- [11] M. A. Ortega-Vazquez and D. S. Kirschen, "Estimating the spinning reserve requirements in systems with significant wind power generation penetration," *IEEE Trans. Power Syst.*, vol. 24, no. 1, pp. 114–124, Feb. 2009.
- [12] Y. Cao, Y. Tan, C. Li, and C. Rehtanz, "Chance-constrained optimization-based unbalanced optimal power flow for radial distribution networks," *IEEE Trans. Power Del.*, vol. 28, no. 3, pp. 1855–1864, Jul. 2013.
- [13] C. Chen, S. Duan, T. Cai, B. Liu, and G. Hu, "Optimal allocation and economic analysis of energy storage system in microgrids," *IEEE Trans. Power Electron.*, vol. 26, no. 10, pp. 2762–2773, Oct. 2011.
- [14] B. F. Hobbs et al., "Analysis of the value for unit commitment of improved load forecasts," *IEEE Trans. Power Syst.*, vol. 14, no. 4, pp. 1342–1348, Nov. 1999.

- [15] D. Liu et al., "A dynamic economic dispatch method considering with the uncertainty and correlation of wind power," in Proc. IEEE Power Energy Soc. Gen. Meeting, National Harbor, MD, USA, 2014, pp. 1–5.
- [16] H. Wu, X. Liu, and M. Ding, "Dynamic economic dispatch of a microgrid: Mathematical models and solution algorithm," *Elect. Power Energy Syst.*, vol. 63, pp. 336–346, Dec. 2014.
- [17] A. Kurita et al., "Multiple time-scale power system dynamic simulation," IEEE Trans. Power Syst., vol. 8, no. 1, pp. 216–223, Feb. 1993.
- [18] B. Zhang, W. Wu, T. Zheng, and H. Sun, "Design of a multi-time scale coordinated active power dispatching system for accommodating large scale wind power penetration," *Autom. Elect. Power Syst.*, vol. 35, no. 1, pp. 1–6, 2011.
- [19] K. Wang et al., "Multi-time scales coordination scheduling of wind power integrated system," in Proc. PES ISGT Asia, Tianjin, China, 2012, pp. 1–4.
- [20] P. Marannino, G. Granelli, M. Montagna, and A. Silvestri, "Different time-scale approaches to the real power dispatch of thermal units," *IEEE Trans. Power Syst.*, vol. 5, no. 1, pp. 169–176, Feb. 1990.
- [21] Y. Lei, X. Han, and D. Yu, "Multi-time scale decision-making method of synergistic dispatch," in *Proc. PES ISGT Asia*, Tianjin, China, 2012, pp. 1–5.
- [22] T. M. Peng, N. F. Hubele, and G. G. Karady, "Advancement in the application of neural networks for short-term load forecast," *IEEE Trans. Power Syst.*, vol. 7, no. 1, pp. 250–257, Feb. 1992.
- [23] Y. Gu and L. Xie, "Early detection and optimal corrective measures of power system insecurity in enhanced look-ahead dispatch," *IEEE Trans. Power Syst.*, vol. 28, no. 2, pp. 1297–1307, May 2013.
- [24] J. Tong and H. Ni, "Look-ahead multi-time frame generator control and dispatch method in PJM real time operations," in *Proc. IEEE Power Energy Soc. Gen. Meeting*, San Diego, CA, USA, 2011, p. 1.
- [25] J. Zhou et al., "Reserve requirement estimation in microgrid considering various uncertain factors," in *Proc. 2013 Chin. Autom. Congr. (CAC)*, 2013, pp. 1–6.
- [26] D. K. Ranaweera, G. G. Karady, and R. C. Farmer, "Economic impact analysis of load forecasting," *IEEE Trans. Power Syst.*, vol. 12, no. 3, pp. 1388–1392, Aug. 1997.
- [27] X.-Y. Ma, Y.-Z. Sun, and H.-L. Fang, "Scenario generation of wind power based on statistical uncertainty and variability," *IEEE Trans. Sustain. Energy*, vol. 4, no. 4, pp. 894–904, Oct. 2013.
- [28] Z. Ziadi et al., "Optimal voltage control using inverters interfaced with PV systems considering forecast error in a distribution system," IEEE Trans. Sustain. Energy, vol. 5, no. 2, pp. 682–690, Apr. 2014.
- [29] R. A. Jabr, "Adjustable robust OPF with renewable energy sources," IEEE Trans. Power Syst., vol. 28, no. 4, pp. 4742–4751, Nov. 2013.
- [30] A. Lorca and X. A. Sun, "Adaptive robust optimization with dynamic uncertainty sets for multi-period economic dispatch under significant wind," *IEEE Trans. Power Syst.*, vol. 30, no. 4, pp. 1702–1713, Jul. 2015.
- [31] J. Zhao, T. Zheng, and E. Litvinov, "Variable resource dispatch through do-not-exceed limit," *IEEE Trans. Power Syst.*, vol. 30, no. 2, pp. 820–828, Mar. 2015.
- [32] Z. Wang and F. L. Alvarado, "Interval arithmetic in power flow analysis," *IEEE Trans. Power Syst.*, vol. 7, no. 3, pp. 1341–1349, Aug. 1992.
- [33] T. Ding *et al.*, "Interval power flow analysis using linear relaxation and optimality-based bounds tightening (OBBT) methods," *IEEE Trans. Power Syst.*, vol. 30, no. 1, pp. 177–188, Jan. 2015.
- [34] R. Doherty and M. O. Malley, "A new approach to quantify reserve demand in systems with significant installed wind capacity," *IEEE Trans. Power Syst.*, vol. 20, no. 2, pp. 587–595, May 2005.
- [35] Q. Cui, J. Shu, X. Zhang, and Q. Zhou, "The application of improved BP neural network for power load forecasting in the island microgrid system," in *Proc. Int. Conf. Elect. Control Eng.*, Yichang, China, 2011, pp. 6138–6141.



Canbing Li (M'06–SM'13) received the B.E. and Ph.D. degrees from Tsinghua University, Beijing, China, in 2001 and 2006, respectively, both in electrical engineering.

He is currently a Professor with Hunan University, Changsha, China.



Xubin Liu (S'14) received the B.E. degree in automation from the College of Electrical Engineering, Northwest University for Nationalities, Lanzhou, China, in 2013. He is currently pursuing the Ph.D. degree in electrical engineering with Hunan University, Changsha, China.



Yijia Cao (M'98–SM'13) received the B.E. degree from Xi'an Jiaotong University, Xian, China, in 1998, and the Master's and Ph.D. degrees from the Huazhong University of Science and Technology, Wuhan, China, in 1990 and 1994, respectively, all in electrical engineering.

He is currently a Professor and the Vice President with Hunan University, Changsha, China.



Peng Zhang (M'07–SM'10) received the Ph.D. degree in electrical engineering from the University of British Columbia, Vancouver, BC, Canada, in 2009.

He was a System Planning Engineer with BC Hydro and Power Authority, Vancouver. He is an Assistant Professor of Electrical Engineering with the University of Connecticut, Storrs, CT, USA. His current research interests include power system resilience and reliability, microgrid, distributed renewable energy systems, and wide area measurement and control.



Haiqing Shi (S'13) received the B.E. and Master's degrees in electrical engineering from the College of Electrical and Information Engineering, Hunan University, Changsha, China, in 2012 and 2015, respectively.



Lingyu Ren (S'13) received the B.Sc. degree in electrical engineering from Shandong University, Jinan, China, in 2010, and the M.Sc. degree in electric power system and automation from the China Electric Power Research Institute, Beijing, China, in 2013. She is currently pursuing the Ph.D. degree in electrical engineering with the University of Connecticut, Storrs, CT, USA.

Her current research interests include microgrid, power system resilience, and distributed optimization.



Yonghong Kuang received the B.E. degree in electronic information from the Hunan University of Science and Technology, Xiangtan, China, in 2003, and the Master's degree in signal and information processing from Nanchang Hangkong University, Nanchang, China, in 2007. She is currently pursuing the Ph.D. degree in electrical engineering with Hunan University, Changsha, China.

Her current research interests include optimal dispatch schedule of microgrid.